CHEMISTRY
A EUROPEAN JOURNAL

DOI: 10.1002/chem.200903151

Dipolar Compounds Containing Fluorene and a Heteroaromatic Ring as the Conjugating Bridge for High-Performance Dye-Sensitized Solar Cells

Chih-Hsin Chen,[a] Ying-Chan Hsu,[a] Hsien-Hsin Chou,[a] K. R. Justin Thomas,[a] Jiann T. Lin,*[a, b] and Chao-Ping Hsu[a]

Abstract: A novel series of dipolar organic dyes containing diarylamine as the electron donor, 2-cyanoacrylic acid as the electron acceptor, and fluorene and a heteroaromatic ring as the conjugating bridge have been developed and characterized. These metal-free dyes exhibited very high molar extinction coefficients in the electronic absorption spectra and have been successfully fabricated as efficient nanocrystalline TiO_2 dye-sensitized solar cells (DSSCs). The solar-energy-to-electricity conversion efficiencies of DSSCs ranged from 4.92 to 6.88%, which reached 68–96% of a standard device of N719 fabricated and measured under the same conditions. With a TiO_2 film thickness of 6 μm, DSSCs based on these dyes had photocurrents surpassing that of the N719-based device. DFT computation results on these dyes also provide detailed structural information in connection with their high cell performance.

Keywords: donor–acceptor systems · energy conversion · fluorenes · solar cells · sulfur heterocycles

Introduction

In recent years, the search for renewable energy has received worldwide attention because of the fast depletion of fossil fuel reserves and global warming as well as environmental pollution problems accompanying fossil fuel consumption. Solar-energy conversion devices that convert photon energy into electricity are very attractive due to the unlimited solar-energy supply. Inorganic semiconductor solar cells, such as silicon solar cells, have been developed over several decades and have important applications, such as satellites and solar houses. However, silicon materials are very expensive and low-cost alternatives, such as organic semiconductors[1] and organic dye-sensitized solar cells (DSSCs),[2] have attracted considerable interest from both academic and industrial communities. To date, polymer-based solar cells can produce a solar-energy-to-electricity conversion efficiency (η) of up to ~5%.[3] In contrast, ruthenium–polypyridyl complex-based DSSCs were reported to have an even higher η value of ~11%.[4]

After Grätzel's seminal reports on a DSSC that utilized a Ru^{II}-based N3 dye,[5] *cis*-$[Ru(SCN)_2L_2]$ (L = 2,2′-bipyridyl-4,4′-dicarboxylate), and a black dye,[6] $[Ru(SCN)_3L]$ (L = 4,4′,4″-tricarboxy-2,2′:6′,2″-terpyridine), a few DSSCs with similar Ru^{II}–bipyridine or terpyridine dyes[7] have been reported with efficiencies higher than 10%, a value close to an amorphous silicon-based photovoltaic cell. There are two important factors contributing to the high performance of the devices: 1) the presence of strong metal-to-ligand charge-transfer (MLCT) absorption extending to >700 nm allows efficient light-harvesting in the red to near IR region and 2) efficient electron transfer from the commonly used electrolyte, I^-, to the ruthenium dye cation.[8] In recent years, metal-free dipolar organic sensitizers have also been actively investigated. Relative to ruthenium dyes, organic compounds have several advantages: 1) they have larger molar extinction coefficients, which is beneficial to light-harvesting, 2) their structural modification is more flexible, and 3) they are of lower cost. Considerable progress has been made on metal-free dipolar organic sensitizers,[9] and recently Wang and co-workers reported an impressive high conversion efficiency of 9.8% with excellent stability for a DSSC based on a metal-free sensitizer.[10] DSSCs that utilize metal-free organic sensitizers, such as coumarin-,[11] indoline-,[12] cyanine-,[13] hemicyanine-,[14] merocyanine-,[15] perylene-,[16]

[a] Dr. C.-H. Chen, Dr. Y.-C. Hsu, Dr. H.-H. Chou, Dr. K. R. J. Thomas, Prof. Dr. J. T. Lin, Prof. Dr. C.-P. Hsu
Institute of Chemistry, Academia Sinica
Taipei, 115 (Taiwan)
Fax: (+886) 2-27831237
E-mail: jtlin@chem.sinica.edu.tw

[b] Prof. Dr. J. T. Lin
Department of Chemistry, National Central University
Chungli, 320 (Taiwan)

Supporting information for this article is available on the WWW under http://dx.doi.org/10.1002/chem.200903151.

thiophene-,[11b,17] and triarylamine-based[18] compounds were reported to have good conversion efficiencies.

In a previous study, we found that DSSCs based on (*E*)-2-cyano-3-(5-{9,9-diethyl-7-[naphthalen-1-yl(phenyl)amino]-9*H*-fluoren-2-yl}thiophen-2-yl)acrylic acid[17b] exhibited an impressive conversion efficiency (>90% of the standard cell from N3). Possibly the high efficiency of the DSSC stems from the high molar extinction coefficient of the electronic absorption band even though the absorption maximum appears at a much shorter wavelength than that of N3. It is our speculation that the diarylamine donor with a fluorenyl conjugation in the sensitizer plays an important role for the high performance of DSSCs. In this paper, we report a series of metal-free dipolar compounds containing fluorene and heteroaromatic rings as the conjugating bridge. The effects of the donor and the conjugating bridge on the photophysical properties of the dyes and on the performance of DSSCs that use these dyes as the sensitizers are discussed.

Results and Discussion

Synthesis of materials: Compounds (**1**–**8**) synthesized in this study are composed of a diarylamine moiety as the electron donor, a conjugating bridge consisting of a fluorenyl unit and a heteroaromatic ring, and 2-cyano-acrylic acid as the electron acceptor and anchoring group to the TiO_2. The synthetic protocols for **2**–**8** are illustrated in Schemes 1 and 2. In Scheme 1, two key steps were adopted to obtain the intermediates that had no internal vinyl unit between the fluorenyl unit and the heteroaromatic ring: 1) selective conversion of one of the aromatic bromides to an arylamine through a Buchwald–Hartwig C–N bond-formation reaction and 2) a Suzuki coupling reaction of the corresponding boron reagent with aryl bromide. Whereas in Scheme 2, the key steps to obtain the intermediates with an internal vinyl unit between the fluorenyl unit and the heteroaromatic ring are: 1) reduction of 7-bromo-9,9-dihexyl-9*H*-fluorene-2-carbaldehyde to the corresponding alcohol by sodium borohydride, 2) treating the alcohol with triphenylphosphonium hydrobromide to form the corresponding phosphonium salt, 3) Wittig reaction of the phosphonium salt with thiophene-2-carbaldehyde or 2-formylthiazole to afford the intermediate with an internal vinyl unit as a mixture of *E* and *Z* isomers, 4) pure *E* isomer was obtained by adding a catalytic amount of iodine into the CH_2Cl_2 solution of the *E*/*Z* mixture in the dark, and 5) palladium-catalyzed Buchwald–Hartwig C–N bond-formation reactions between arylbromides and diarylamines. All the intermediates were further formylated then reacted with cyanoacetic acid in glacial acetic acid by a Knoevenagel reaction to form the desired products. The coupling constant (J ~15.7 Hz) between the two vicinal vinyl protons in the ^{1}H NMR spectra unambiguously identifies the *E* configuration of the dyes. The dyes are dark-brown and -purple powders, respectively, and are readily soluble in common organic solvents, such as THF, CH_2Cl_2, and $CHCl_3$.

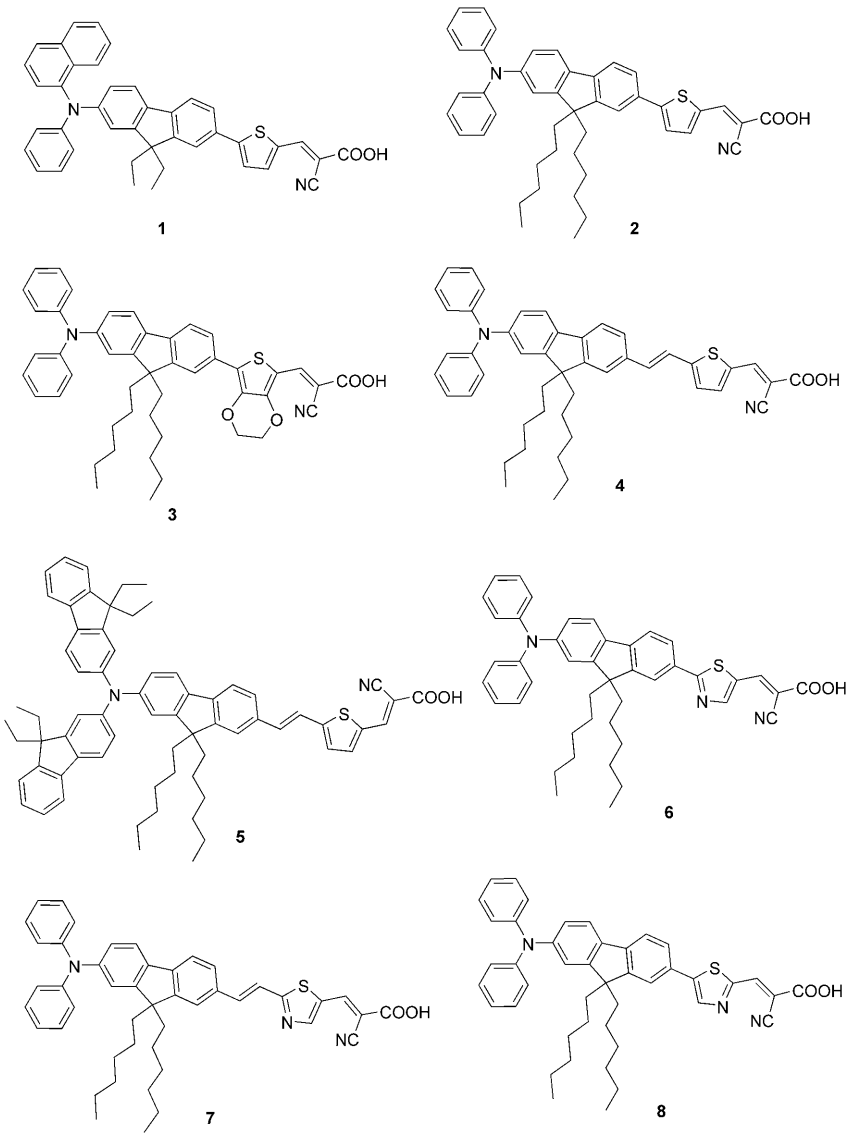

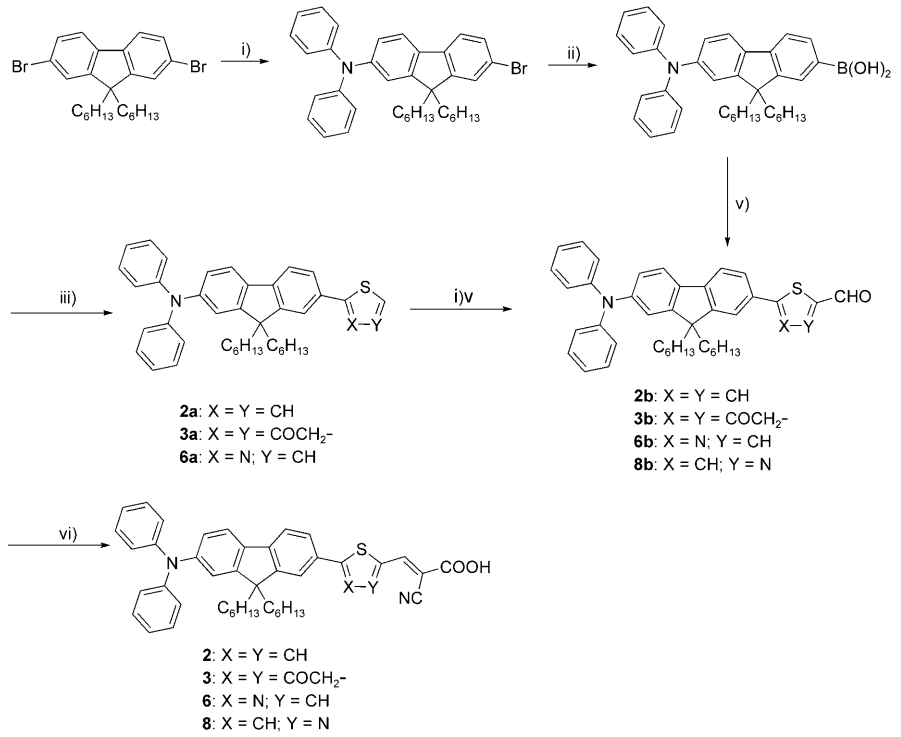

Scheme 1. Synthetic route for **2**, **3**, **6**, and **8**: i) diphenylamine, $[Pd(dba)_2]$ (dba = bis(dibenzylideneacetone), 1,1′-bis(diphenylphosphino)ferrocene (dppf), *t*BuONa, toluene; ii) *n*BuLi, $B(OMe)_3$; iii) 2-bromothiophene, 5-bromo-2,3-dihydrothieno[3,4-*b*-1,4]dioxine or 2-bromothiazole, $[Pd(PPh_3)_4]$, Na_2CO_3 (2 M, aq), toluene; iv) *n*-BuLi, DMF or *n*-formylmorpholine; v) 2-(1,3-dioxolan-2-yl)-5-iodothiazole, $[Pd(PPh_3)_4]$, Na_2CO_3 (2 M, aq), toluene, then acetic acid; vi) 2-cyanoacetic acid/NH_4OAc/acetic acid.

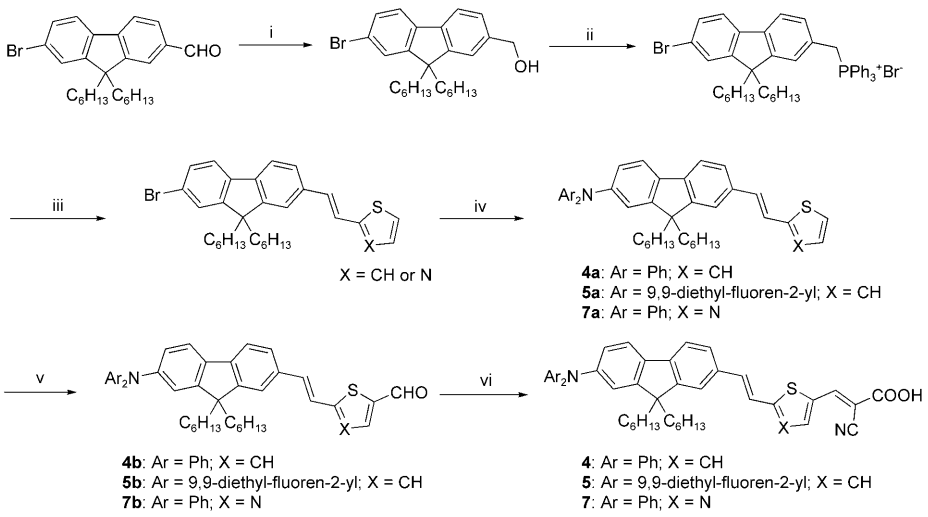

Scheme 2. Synthetic route for **4**, **5**, and **7**: i) $NaBH_4$, THF; ii) $HPPh_3Br$, $CHCl_3$; iii) a) thiophene-2-carboxaldehyde or 2-formylthiazole, *t*BuOK, THF; b) I_2, CH_2Cl_2; iv) diphenylamine or *N*,*N*-bis(9,9-diethyl-9*H*-fluoren-2-yl)amine, $Pd(OAc)_2$, $P(tBu)_3$, *t*BuONa, toluene; v) *n*BuLi, DMF or *n*-formylmorpholine, THF; vi) 2-cyanoacetic acid, NH_4OAc, acetic acid.

Photophysical properties: The absorption spectra of the dyes in THF are shown in Figure 1 and the photophysical data are collected in Table 1. The band ranging from 300–400 nm (band I) can be attributed to the localized π–π* transition, whereas the band at >400 nm (band II) is likely due to the charge-transfer transition mixed with more delocalized π–π* transitions. The charge-transfer character of the longer wavelength absorption is supported by the following observations: replacement of the 2-cyanoacrylic acid moiety in **7** by a formyl group and a hydrogen atom, respectively, leads to a decreasing of λ_{max} by 40 nm (467 vs. 427 nm in THF) and 69 nm (467 vs. 398 nm in THF). The energy of the band II is dependent on the spacer used. For example, the charge-transfer and/or the π–π* transition decrease in energy when an ethylene unit is inserted between the fluorene moiety and the heteroaromatic ring, that is, $\lambda_{max}(\mathbf{2}) < \lambda_{max}(\mathbf{4})$ and $\lambda_{max}(\mathbf{6}) < \lambda_{max}(\mathbf{7})$. Consistent with literature reports,[19] the thiazole moiety was found to be beneficial in lowering the energy of the charge-transfer transition, that is, $\lambda_{max}(\mathbf{8}) \approx \lambda_{max}(\mathbf{6}) > \lambda_{max}(\mathbf{2})$. It is interesting to note that the molar extinction coefficient of the thiazole derivative is lower than that of the thiophene congener if the heteroatoms are closer to the acceptor (2-cyanoacrylic acid), that is, $\varepsilon(\mathbf{8}) < \varepsilon(\mathbf{2})$. On the contrary, the thiazole compound has a higher molar extinction coefficient if the heteroatoms are away from the acceptor, that is, $\varepsilon(\mathbf{2}) < \varepsilon(\mathbf{6})$.

Similar to some metal-free dipolar sensitizers,[17c,g] a blueshift of the charge-transfer band in a more polar solvent, that is, negative solvatochromism, is detected in these compounds. For example, the λ_{max} value decreases by 20 nm on going from THF to CH_3CN. This may be attributed to the strong interaction of polar solvent molecules with the sensitizer, which weakens the O–H bond of the carboxylic acid and consequently decreases the electron-withdrawing nature of the COOH group.[17g,18d] Similar behavior was reported in the ruthenium-containing black dye.[6]

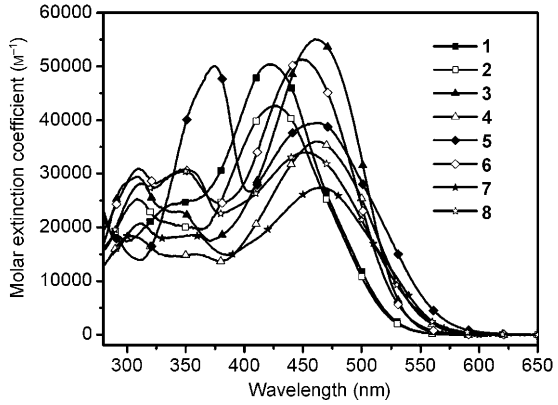

Figure 1. Absorption spectra of dyes recorded in THF.

Table 1. Electrooptical parameters of the dyes.

Dye	λ_{abs} ($\varepsilon\times10^{-4}$ M^{-1}cm^{-1})[a] [nm]	$E_{1/2}$ (ΔE_p)[b] [mV]	HOMO/LUMO [eV]	E_{0-0}[c] [eV]	E_{0-0}*[d] [V]
1	421 (5.29), 333 (1.39)	435 (65)	5.24/2.66	2.58	−1.44
2	427 (4.26), 348 (2.04), 308 (2.52)	419 (94)	5.22/2.84	2.38	−1.26
3	460 (5.51), 343 (2.03), 309 (2.94)	390 (69)	5.19/2.87	2.32	−1.23
4	462 (3.60), 358 (1.51), 302 (1.84)	375 (76), 888 (106)	5.18/2.93	2.25	−1.17
5	461 (3.94), 374 (5.00)	242 (78), 841 (120)	5.04/2.85	2.19	−1.25
6	448 (5.13), 348 (3.08), 310 (3.10)	456 (92)	5.26/2.93	2.33	−1.17
7	467 (2.74), 355 (1.86), 312 (2.07)	407 (84)	5.21/3.00	2.21	−1.10
8	452 (3.39), 352 (3.07), 313 (2.82)	435 (100)	5.24/2.92	2.32	−1.18

[a] Recorded in THF. [b] Recorded in CH_2Cl_2. scan rate = 100 mV s^{-1}; electrolyte = $(n\text{-}C_4H_9)_4NPF_6$; ΔE_p is the separation between the anodic and cathodic peaks. Potentials are quoted with reference to the internal ferrocene standard ($E_{1/2}$ = +212 mV vs $Ag/AgNO_3$). [c] The bandgap, E_{0-0}, was derived from the observed optical edge. [d] E_{0-0}*: the excited-state oxidation potential vs. NHE.

Electrochemical properties: The electrochemical properties of the dyes were studied by cyclic voltammetry (CV) and differential pulse voltammetry (DPV). Representative cyclic voltammograms are shown in Figure 2 and the relevant CV data are collected in Table 1. All dyes exhibit a quasi-reversible one-electron redox wave (242–456 mV vs Fc/Fc^+) attributed to the oxidation of the arylamine. The oxidation potentials (E_{ox}) of the compounds decrease in the order of **6** > **8** ≈ **1** > **2** > **7** > **3** > **4** > **5**. The very low oxidation potential in **5** is consistent with our previous observation that the electron-excessive fluoren-2-yl moiety can significantly increase the electron density at the attached nitrogen atom.[20] The heteroaromatic ring in the spacer also affects the oxidation potential of the arylamine, and the electron-deficient thiazole moiety results in a higher E_{ox} value relative to the electron-excessive thiophene moiety, that is, $E_{ox}(\mathbf{6}) > E_{ox}(\mathbf{2}) > E_{ox}(\mathbf{3})$. Moreover, the shorter distance between the amine and the thiazole leads to a higher E_{ox} value: **6** > **7**. It is conceivable that electron injection from the excited dye to TiO_2 is energetically favored since the excited-state potential (E_{0-0}*) of the sensitizer, estimated from the difference between the first oxidation potential at the ground state and the zero–zero excitation energy E_{0-0}, is more negative (−1.10 to −1.44 V vs NHE, see Table 1) than the conduction-band-edge energy level of the TiO_2 electrode, −0.5 V vs NHE.[21] Dye regeneration should also be energetically favored in view that the first oxidation potentials of the dyes (0.94 to 1.16 V vs NHE) are more positive than that of the I^-/I_3^- redox couple (0.4 V vs NHE).[17g,22]

Photovoltaic devices: Dye-sensitized solar cells with an effective area of 0.25 cm^2 were fabricated by using the compounds adsorbed on nanocrystalline anatase TiO_2 as the sensitizers and an acetonitrile solution containing I_2 (0.05 M)/LiI (0.5 M)/*tert*-butyl pyridine (0.5 M) as the electrolyte. The device performance statistics under AM 1.5 illumination are collected in Table 2. The photocurrent-voltage (J-V) curves and the incident photon-to-current conversion efficiencies (IPCE) of the cells are plotted in Figures 3 and 4, respectively. All the devices showed moderate to good power conversion efficiencies ranging from 4.92 to 6.88%. These values correspond to 68–96% of the standard cell of ruthenium dye N719 fabricated and measured under similar conditions. The impressively high conversion efficiencies of several devices can be attributed to the very high molar extinction coefficients of the dye (ε > 35000 M^{-1}cm^{-1} except **7** and **8**), which well exceed 20000 M^{-1}cm^{-1}, an uppermost value observed for most ruthe-

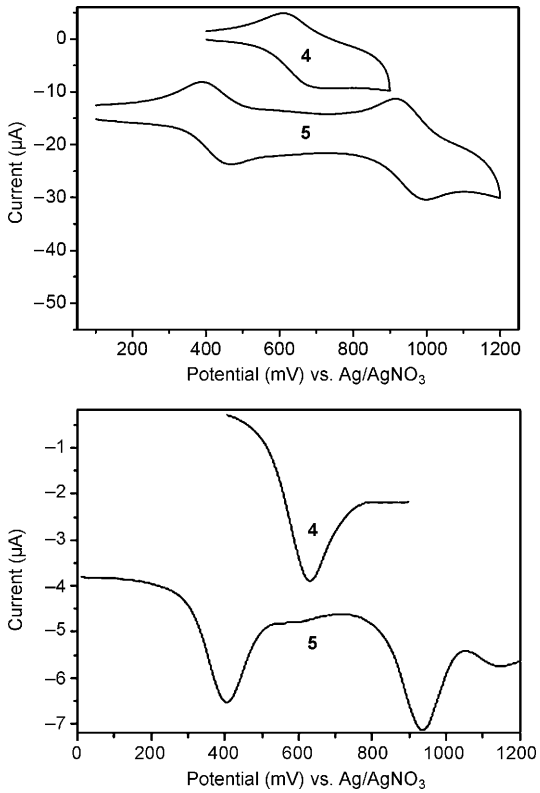

Figure 2. Cyclic voltammograms of **4** and **5** recorded in CH_2Cl_2 (scan rate: 100 mV s^{-1} (top). Differential pulse voltammograms in the oxidation region (bottom).

Table 2. Performance parameters of DSSCs based on dyes **1**–**8** and N719.[a]

Dye	J_{sc} [mA cm^{-2}]	V_{oc} [V]	FF	η [%]
1	16.06	0.67	0.64	6.76
2	15.82	0.68	0.63	6.78
3	14.32	0.68	0.64	6.23
4	15.67	0.65	0.64	6.46
5	13.65	0.64	0.67	5.78
6	14.55	0.71	0.67	6.88
7	13.66	0.67	0.64	5.83
8	10.40	0.66	0.72	4.92
N719	16.08	0.72	0.63	7.19

[a] Experiments were conducted by using TiO_2 photoelectrodes with approximately 16 μm thickness and a 0.25 cm^2 working area on the FTO (15 Ω/sq.) substrates.

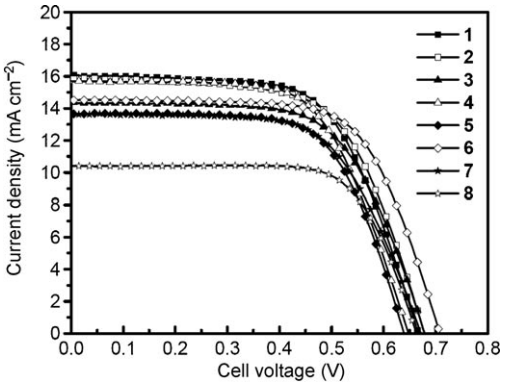

Figure 3. J-V curves of DSSCs based on the dyes **1**–**8**.

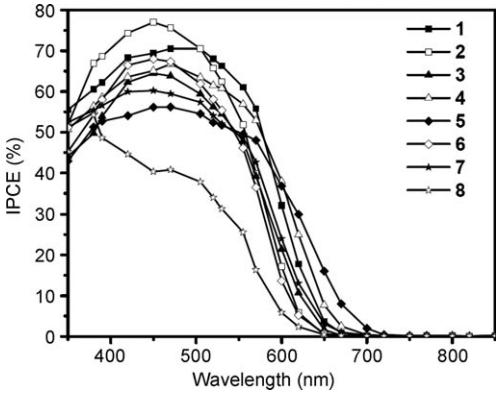

Figure 4. IPCE plots for the DSSCs by using dyes **1**–**8**.

nium-based sensitizers.[5–7] Consequently, strong absorption appears to compensate well for the much shorter absorption wavelength of the metal-free dyes relative to the ruthenium-based sensitizers.

The adsorbed densities of the dyes on the TiO_2 surface were checked (**1**: 2.7×10^{-7}, **2**: 2.5×10^{-7}, **3**: 2.8×10^{-7}, **4**: 3.0×10^{-7}, **5**: 7.9×10^{-8}, **6**: 2.9×10^{-7}, **7**: 3.3×10^{-7}, **8**: 2.7×10^{-7} mol cm^{-2}) and found to differ within 25% except for **5**. The smaller density of **5** is likely due to the greater steric congestion of the two fluorenyl moieties at the donor. Comparatively lower conversion efficiencies and smaller short-circuit currents (J_{SC}) in **8**-based DSSCs can be attributed to the less efficient light harvesting of the sensitizers after being adsorbed on the TiO_2 surface. Though high-performance DSSCs were reported for sensitizers containing the bis(fluoren-2-yl)amino donor,[17f,18b,c] sensitizer **5** with such a moiety was found to have a device efficiency inferior to **2**, which contains a diphenylamino donor. Relative to **2**, both J_{SC} and V_{OC} (open-circuit voltage) dropped in the **5**-based cell. The shorter recombination lifetime of the photoinjected electrons with the oxidized dye (vide infra) and the smaller adsorption density of **5** may be the main cause of the lower photocurrent of the device. The higher-lying HOMO of **5** may also decrease the driving force of dye regeneration by the electrolyte, I^-/I_3^-. Accordingly, more competitive recombination (vide infra) of the photoinjected electrons with oxidized dye and oxidized mediator will lead to decreased V_{OC} and J_{SC}. The lower V_{OC} value of the **5**-based DSSC is supported by its higher dark current (see Figure S1 in the Supporting Information). DSSCs of **4** with a similarly high dark current also had a relatively low V_{OC}. DSSCs based on **6** have the highest conversion efficiency (6.88%) of all. This outcome is attributed to four factors: 1) compound **6** has a high molar extinction coefficient and long absorption wavelength, 2) the cell has an impressively high V_{OC} value, 3) the cell has the longest recombination lifetime of the photoinjected electrons with the oxidized dye (vide infra), and 4) the cell has the lowest dark current. It is important to note that the heteroaromatic ring in the conjugating bridge is very critical for the high performance of DSSCs in this study. For example, compound **1′** formed by stripping off the thiophene ring from **1** has a device efficiency at least 10% lower than that of **1**.[23] A significantly larger molar extinction coefficient of **1** than **1′** (52900 vs. ~26000 M^{-1}cm^{-1}) clearly results in better light-harvesting of the former even though the two dyes have comparable absorption wavelengths. The importance of the fluorenyl unit for the high performance of the cells is also realized from the following observations: 1) **1** has a larger molar extinction coefficient than its congener in which the fluorenyl entity is replaced by a biphenyl entity, (*E*)-2-cyano-3-{5′-[4″-(naphthylphenylamino)biphenylene]thiophen-2′-yl}acrylic acid,[24] and the former has device efficiency 20% higher than that of the latter, 2) when the fluorenyl entity of **2** is replaced with a phenyl entity, the resulting compound, 5-[4-(diphenylaminophenyl)]thiophene-2-cyanoacrylic acid, has a device efficiency ~27% lower than that of **2**.[25] A significantly larger molar extinction coefficient was also noticed in the compound with the fluorenyl entity, **1**. Insertion of a vinyl entity between the fluorene unit and the heteroaromatic ring leads to a redshift of the absorption band at the expense of cell efficiency, that is, (**4**) < (**2**) and (**7**) < (**6**). The much shorter recombination lifetime of the photoinjected electrons with the oxidized dye is likely an important factor leading to lower efficiencies of DSSCs based on sensitizers with a vinyl entity, **4**, **5**, and **7**. However, more studies are needed to elucidate the role of the vinyl entity. Increasing the number of the thienylfluorene segments also results in the inferior effi-

ciency of the DSSC because of the deviation of the two successive aromatic segments from coplanarity for the dyes with a longer spacer.[17b]

The recombination lifetime of the photoinjected electron (τ_R) with the oxidized dye was measured by a transient photovoltage at open circuit. The electrolyte used was 0.5 M of $LiClO_4$ or LiI in CH_3CN. I_2 was omitted to avoid the possibility of a dark current. The resulting τ_R values are listed in Table 3. The τ_R values are comparable and range from 0.16 to 0.20 ms in the presence of $LiClO_4$. However, they are slightly smaller than that of the N719-based device. In the presence of LiI, regeneration of the sensitizer by the electrolyte retards the recombination and significantly increases τ_R values, ranging from 1.49 to 10.30 ms relative to 8.83 ms for the N719-based device. The longest electron lifetime found in **6** is consistent with the highest V_{OC} value for the **6**-based cell. The shortest lifetime in **5** is attributed to the slower dye regeneration because of the higher HOMO level of the dye (vide supra). In addition, when the vinyl group is inserted into the spacer, both τ_R and V_{OC} values decrease, that is, $\tau_R(\mathbf{2}) > \tau_R(\mathbf{4})$ and $V_{OC}(\mathbf{2}) > V_{OC}(\mathbf{4})$. The same trend was also found for compounds **6** and **7**.

Table 3. Recombination lifetime of the photoinjected electrons.

Dye	**1**	**2**	**3**	**4**	**5**	**6**	**7**	**8**	N719
τ_R [ms]	9.43	6.37	4.63	3.85	1.49	10.30	4.86	6.07	8.83

The use of thinner films of TiO_2 is demanding for DSSCs employing solvent-free ionic liquid electrolytes or solid-state organic hole-transporting materials because of the limited electron diffusion length.[26] However, optical absorption will be sacrificed with the use of the thinner TiO_2 film. It is possible to settle this dilemma if the sensitizers possess sufficiently high molar extinction coefficients. Sensitizers **1** and **6** possessing high molar extinction coefficients were, therefore, tested for DSSCs with thinner sensitized-TiO_2 films. The performance parameters of the DSSCs with TiO_2 films of different thickness are listed in Table 4. With the thicknesses of the TiO_2 films at 6 μm, both the photocurrents and the power conversion efficiencies of devices that utilize **1** and **6** were larger than that of the N719-based device. In the region between 500 and 350 nm the IPCEs of **1** and **6** clearly exceeded that of N719 (Figure 5). There should be the opportunity of panchromatic co-sensitization by using **1** or **6** with a sensitizer absorbing in the near-IR region.[27]

Table 4. Performance parameters of the DSSCs fabricated with different TiO_2 films.

Thickness	Dye	V_{OC} [V]	J_{SC} [mA cm^{-2}]	η [%]	FF
6 μm[a]	**1**	0.69	13.53	6.15	0.66
	6	0.72	11.85	5.89	0.70
	N719	0.76	11.48	5.79	0.66
10 μm[a]	**1**	0.68	14.47	6.38	0.65
	6	0.71	13.02	6.38	0.69
	N719	0.73	13.62	6.63	0.67

[a] Without a 300 nm-sized light-scattering layer.

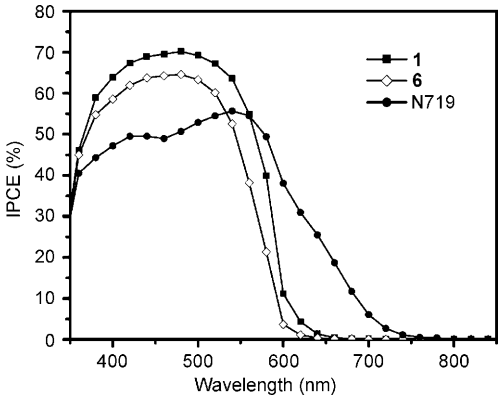

Figure 5. IPCE of the DSSCs fabricated with 6 μm TiO_2 films by using dyes **1**, **6**, and N719.

Theoretical approach: To gain insight into the relationship between the structure and photophysical properties of the dyes, some density functional calculations at the B3LYP/6-31G* level were conducted. The computed frontier orbitals of the compounds and their corresponding energy states are included in Figure S2 (see the Supporting Information) and Figure 6, respectively. In the optimized structure, no significant deviation from planarity was found in the spacer between the arylamine and 2-cyanoacrylic acid (see Figure S3 in the Supporting Information). The dihedral angles between any two neighboring segments are $\leq 3.0°$ for compounds **1**, **2**, **4**, **5**, and **7**. In comparison, compounds with a thiazolyl (abbreviated as Tha) or substituted thiophene (abbreviated as edoT) group have a larger dihedral angle between the fluorenyl segment (abbreviated as Flu) and the heteroaromatic ring, ranging from 16.1 to 21.3° (compounds **3**, **6**, and **8**). Further TD-DFT calculations of the dyes at the same level were also performed (see the Experimental Section), and the results are listed in Table S1 (see the Supporting Information). The HOMO and HOMO−1 orbitals in

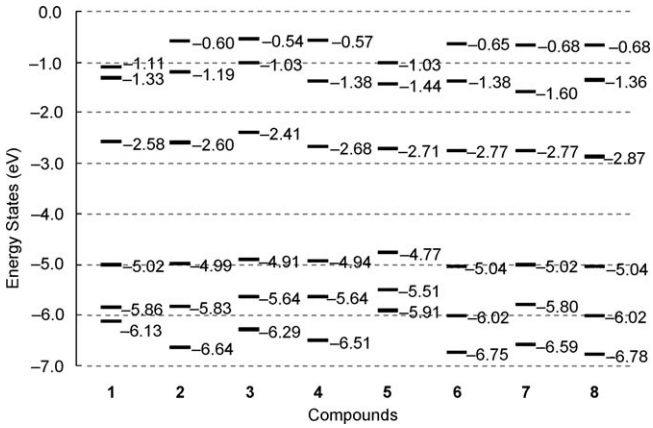

Figure 6. Computed energy states of the compounds.

these compounds are mainly composed of the diarylamine and fluorenyl fragments, with some contribution from the vinyl entity and the heteroaromatic ring. In comparison, the LUMO and LUMO+1 orbitals are mainly composed of the heteroaromatic ring and a 2-cyanoacrylic acid moiety, with some contribution from one of the phenyl rings in the fluorenyl fragment and the vinyl entity. Consistent with the electrochemical data, compound **5** containing a more electron-releasing bis(trifluorenyl)amino group was calculated to have the highest HOMO energy level, −4.77 eV. For all molecules, the S_1 state consists of a HOMO→LUMO transition exclusively, whereas the S_2 state consists mainly of a HOMO−1→LUMO transition (76–95%). Both transitions are typical π–π* transitions with charge-transfer character. Based on the calculated oscillator strength, it is likely that the observed band with the lowest energy is a combination of $S_0 \rightarrow S_1$ and $S_0 \rightarrow S_2$ transitions. The calculated excitation energies of the vinyl-free dyes are in the order of **1**-(2.24 eV) > **2**(2.16 eV) > **6**(2.08 eV) > **8**(1.98 eV), and the trend is in parallel with the spectroscopic data. For the dyes containing an internal vinyl entity, that is, **4**, **5**, and **7**, their corresponding energy gaps are smaller than those of the vinyl-free analogues due to the elongated π-conjugation.

The Mulliken charges for the S_1, S_2, and S_3 states were also calculated from the TD-DFT results. Differences in the Mulliken charges in the excited and ground states were calculated and grouped into several segments, diarylamine (Am, Am′, or Am″), fluorene (Flu or Flu′), vinyl (v), heteroaromatic ring (T, edoT, Tha, or Tha′), and 2-cyanoacrylic acid (Ac), to estimate the extent of charge separation upon excitation (see Table S1 in the Supporting Information). Figure S4 (see the Supporting Information) displays the changes in Mulliken charges of the dyes for the $S_0 \rightarrow S_1$ and $S_0 \rightarrow S_2$ transitions. In general, there is significant charge transfer from the arylamine donor to the 2-cyanoacrylic acid acceptor for all $S_0 \rightarrow S_n$ ($n = 1$–3) transitions, that is, significant positive and negative charges are located at the donor and acceptor, respectively. The negative charge accumulated at 2-cyanoacrylic acid (Ac) was found to be larger in the vinyl-free dyes **1**, **2**, **3**, **6**, and **8** (−0.37–0.44) than that in the others (−0.32–0.34 for **4**, **5**, and **7**). For the $S_0 \rightarrow S_1$ and $S_0 \rightarrow S_2$ transitions of dyes **6**, **7**, and **8**, the electron-withdrawing nature of thiazolyl group (Tha) is evident from their greater accumulation of Mulliken charges (−0.28–0.33 for $S_0 \rightarrow S_1$; −0.13–0.15 for $S_0 \rightarrow S_2$) than the corresponding thienyl analogues.

It is interesting to note that sensitizer **8**, with heteroatoms on the thiazole ring closer to the acceptor, has significantly lower device efficiency than its isomer **6**, containing heteroatoms away from the acceptor, after the dye concentration on TiO_2 is corrected. This outcome can be rationalized by two factors: 1) there is better light-harvesting for **6** and 2) compound **6** has a longer electron recombination lifetime. It is known that the work function of the semiconductor can be tuned by the interface dipole created by the organic molecules anchored at the surface of the semiconductor.[28] We speculate that the different orientation of the thiazolyl ring leads to a different surface dipole of TiO_2 and affects the tendency of electron recombination.

Conclusion

In summary, we have synthesized a class of dipolar compounds containing a fluorenyl segment and a heteroaromatic ring as the conjugating bridge. These metal-free sensitizers could be efficiently adsorbed on nanocrystalline anatase TiO_2 particles for the dye-sensitized solar cells application. The very strong absorption of the dyes results in favorable light harvesting and a high performance of the DSSCs has been achieved. The maximum solar-energy-to-electricity conversion efficiency under AM 1.5 irradiation is 6.88%, reaching 96% of the standard cell of ruthenium dye N719 fabricated and measured under similar conditions. Density functional studies provided further support on the high cell performance of these dyes. DSSCs with a thinner film of TiO_2 had photocurrents surpassing that of the N719-based device, which will pave the way for a future panchromatic approach using co-sensitizers or an application in solid-state DSSCs.

Experimental Section

General information: Unless otherwise specified, all the reactions were performed under a nitrogen atmosphere by using standard Schlenk techniques. THF was distilled from sodium and benzophenone under a nitrogen atmosphere. DMF and CH_2Cl_2 were distilled from CaH_2 under a nitrogen atmosphere. The synthesis of starting materials and intermediates are described in the Supporting Information. The synthesis of **1** was described in our previous study.[17b] All chromatographic separations were carried out on silica gel (60 M, 230–400 mesh). ^1H and ^{13}C NMR spectra were recorded on a Bruker AMX400 or AV500 spectrometer. Mass spectra (FAB) were recorded on a VG70–250S mass spectrometer. Elementary analyses were performed on a Perkin–Elmer 2400 CHN analyzer. Cyclic voltammetry experiments were performed with a CH Instruments electrochemical analyzer. All measurements were carried out at room temperature with a conventional three electrode configuration consisting of a platinum working electrode, a platinum wire auxiliary electrode, and a nonaqueous $Ag/AgNO_3$ reference electrode. The $E_{1/2}$ values were determined as $(E_{pa}+E_{pc})/2$, in which E_{pa} and E_{pc} are the anodic and cathodic peak potentials, respectively. The potentials are quoted against the ferrocene internal standard. The solvent used in all experiments was THF, and the supporting electrolyte was 0.1 M tetrabutylammonium hexafluorophosphate. Electronic absorption spectra were obtained on a Cary 50 Probe UV/Vis spectrophotometer.

Synthesis of 2a–7a: The syntheses of compounds **2a**, **3a**, and **6a** and compounds **4a**, **5a**, and **7a** follow similar procedures. Therefore, only the synthesis of **2a** and **4a** will be described in detail. The characterization details for other compounds are provided in the Supporting Information.

9,9-Dihexyl-*N*,*N*-diphenyl-7-(thiophen-2-yl)-9*H*-fluoren-2-amine (2a): Dry toluene (40 mL) was added to a flask containing a mixture of 7-(diphenylamino)-9,9-dihexyl-9*H*-fluoren-2-yl-boronic acid (2.40 g, 4.4 mmol), 2-bromothiophene (0.65 g, 4.0 mmol), Na_2CO_3 (2 M in H_2O, 8.0 mL, 16.0 mmol), and $[Pd(PPh_3)_4]$ (0.19 g, 0.16 mmol). After the reaction mixture had been refluxed for 24 h, the solvent was removed and the residue was extracted with CH_2Cl_2/brine. The organic layer was dried over anhydrous $MgSO_4$, then filtered and dried. The crude product was further purified by column chromatography by using CH_2Cl_2/hexanes (1:2) as the eluent to give **2a** as a pale-yellow solid (2.1 g, 68%).

^{1}H NMR ($CDCl_3$): δ = 7.61–7.58 (m, 2H), 7.52–7.44 (m, 3H), 7.25–7.21 (m, 5H), 7.10–7.06 (m, 5H), 7.00–6.93 (m, 4H), 1.88–1.83 (m, 4H), 1.24–1.09 (m, 12H), 0.75 (t, J = 7.1 Hz, 6H), 0.70–0.60 ppm (m, 4H); FAB-MS: m/z: 583.4 [M^+].

(*E*)-9,9-Dihexyl-*N*,*N*-diphenyl-7-[2-(thiophen-2-yl)vinyl]-9*H*-fluoren-2-amine (4a): A mixture of diphenylamine (0.19 g, 1.1 mmol), 2-[2-(7-bromo-9,9-dihexyl-9*H*-fluoren-2-yl)vinyl]thiophene (0.52 g, 1.0 mmol), sodium *tert*-butoxide (0.14 g, 1.5 mmol), $Pd(OAc)_2$ (4.5 mg, 0.02 mmol), tri(*tert*-butyl)phosphine (5.5 mg, 0.02 mmol), and dry toluene (20 mL) was refluxed under nitrogen for 16 h. After cooling, the reaction mixture was quenched with water and the mixture was extracted with CH_2Cl_2. The combined organic layer was washed with brine and dried over anhydrous $MgSO_4$. After filtration and removal of the solvent, the crude product was further purified by column chromatography by using CH_2Cl_2/hexane (1:1) as the eluent to yield **4a** as a pale-yellow oil (0.43 g, 70%). ^{1}H NMR ($CDCl_3$): δ = 7.70 (d, J = 8.4 Hz, 2H), 7.66 (s, 1H), 7.53 (dd, J = 8.0, 1.6 Hz, 1H), 7.48 (d, J = 16.0 Hz, 1H), 7.35 (d, J = 5.2 Hz, 1H), 7.31–7.26 (m, 4H), 7.18–7.16 (m, 2H), 7.08–7.01 (m, 9H), 1.90–1.80 (m, 4H), 1.12–1.02 (m, 12H), 0.78 (t, J = 7.2 Hz, 6H), 0.70–0.64 ppm (m, 4H); FAB-MS: m/z: 609.9 [M^+].

Synthesis of 2b–8b: The syntheses of compounds **2b**–**5b** and compounds **6b** and **7b**, follow similar procedures. Therefore, only the synthesis of **2b**, **6b**, and **8b** will be described in detail. The characterization details for the other compounds are provided in the Supporting Information.

5-[7-(Diphenylamino)-9,9-dihexyl-9*H*-fluoren-2-yl]thiophene-2-carbaldehyde (2b): *n*BuLi (1.6 M in hexane, 1.38 mL, 2.2 mmol) was added dropwise at −78 °C to a solution of **2a** (1.17 g, 2.0 mmol) in anhydrous THF (10 mL). After the solution had been stirred at −78 °C for 1 h, dry DMF (1 mL) was added slowly. After the addition, the solution was stirred at −78 °C for 30 min, then warmed to room temperature and stirred overnight. The reaction was quenched by the addition of dilute HCl aqueous solution and the mixture was extracted with CH_2Cl_2. The combined organic layer was washed with brine and dried over anhydrous $MgSO_4$. After filtration and removal of the solvent, the crude product was further purified by column chromatography by using CH_2Cl_2/hexanes (1:1) as the eluent to yield **2b** as a yellow solid (0.89 g, 73%). ^{1}H NMR ($CDCl_3$): δ = 9.87 (s, 1H), 7.73 (d, J = 4.0 Hz, 1H), 7.64–7.61 (m, 2H), 7.55–7.53 (m, 2H), 7.42 (d, J = 4.0 Hz, 1H), 7.25–7.21 (m, 4H), 7.11–7.08 (m, 5H), 7.02–6.98 (m, 3H), 1.88–1.84 (m, 4H), 1.23–1.09 (m, 12H), 0.75 (t, J = 7.1 Hz, 6H), 0.70–0.60 ppm (m, 4H); FAB-MS: m/z: 611.3 [M^+].

2-[7-(Diphenylamino)-9,9-dihexyl-9*H*-fluoren-2-yl]thiazole-5-carbaldehyde (6b): *n*BuLi (1.6 M in hexane, 1.38 mL, 2.2 mmol) was added dropwise at −78 °C to a solution of **6a** (1.17 g, 2.0 mmol) in anhydrous THF (10 mL). The solution was stirred at −78 °C for 1 h, then a solution of *N*-formylmorpholine (0.30 mL, 3.0 mmol) in anhydrous THF (10 mL) was added slowly. After the addition, the solution was stirred at −78 °C for 30 min, then warmed to room temperature and stirred overnight. Saturated NH_4Cl solution was added and the solution was stirred at room temperature for 15 min. The organic phase was separated and the aqueous layer was extracted with CH_2Cl_2. The combined organic layer was washed with brine and dried over anhydrous $MgSO_4$. After filtration and removal of the solvent, the crude product was further purified by column chromatography by using CH_2Cl_2/hexanes (3:2) as the eluent to yield **6b** as a yellow solid (0.86 g, 70%).

5-[7-(Diphenylamino)-9,9-dihexyl-9*H*-fluoren-2-yl]thiazole-2-carbaldehyde (8b): Dry toluene (40 mL) was added to a flask containing a mixture of 7-(diphenylamino)-9,9-dihexyl-9*H*-fluoren-2-yl boronic acid (2.40 g, 4.4 mmol), 2-(1,3-dioxolan-2-yl)-5-iodothiazole (1.13 g, 4.0 mmol), Na_2CO_3 (2 M in H_2O, 8.0 mL, 16.0 mmol), and $[Pd(PPh_3)_4]$ (0.19 g, 0.16 mmol). After the reaction mixture had been refluxed for 24 h, the solvent was removed and the residue was extracted with CH_2Cl_2/brine. The organic layer was dried over anhydrous $MgSO_4$, then filtered and pumped dry. Glacial acetic acid (25 mL) was added to the crude product and the mixture was heated to 50 °C. After the solution turned clear, water (4 mL) was added and the solution was stirred at 50 °C for another 3 h. The solution was cooled and iced water (50 mL) was added. The precipitate formed was filtered, washed with water and methanol, and then dried. The crude product was further purified by column chromatography by using CH_2Cl_2/hexanes (1:1) as the eluent to give **8b** as a pale-yellow solid (1.35 g, 55%). ^{1}H NMR ($CDCl_3$): δ = 9.95 (s, 1H), 8.29 (s, 1H), 7.63 (d, J = 8.0 Hz, 1H), 7.59 (dd, J = 8.0, 1.6 Hz, 1H), 7.55 (d, J = 8.0 Hz, 1H), 7.50 (d, J = 1.2 Hz, 1H), 7.26–7.22 (m, 4H), 7.12–7.08 (m, 5H), 7.03–6.99 (m, 3H), 1.90–1.83 (m, 4H), 1.12–1.04 (m, 12H), 0.77 (t, J = 7.2 Hz, 6H), 0.70–0.63 ppm (m, 4H); FAB-MS: m/z: 612.2 [M^+].

Synthesis of compounds 2–8: Compounds **2**–**8** were synthesized by similar procedures. Only the synthesis of **2** will be described in detail. The characterization details for other compounds are provided in the Supporting Information.

(*E*)-2-Cyano-3-{5-[7-(diphenylamino)-9,9-dihexyl-9*H*-fluoren-2-yl]thiophen-2-yl} acrylic acid (2): Acetic acid (10 mL) was added to a mixture of 5-[7-(diphenylamino)-9,9-dihexyl-9*H*-fluoren-2-yl]thiophene-2-carbaldehyde (0.61 g, 1.0 mmol), cyanoacetic acid (0.085 g, 1.0 mmol), and ammonium acetate (0.019 g, 0.25 mmol). The mixture was heated at 120 °C for 16 h and then allowed to cool to room temperature. Water was added and the resulting solid was filtered and washed with water to afford the crude product. It was further purified by column chromatography on silica gel by using CH_2Cl_2 then CH_2Cl_2/acetic acid (5:1) as the eluents to yield **2** as a dark-red solid (0.45 g, 66%). ^{1}H NMR ($CDCl_3$): δ = 8.34 (s, 1H), 7.89 (d, J = 4.0 Hz, 1H), 7.67 (d, J = 8.0 Hz, 1H), 7.61 (d, J = 8.0 Hz, 1H), 7.54–7.57 (m, 2H), 7.48 (d, J = 4.0 Hz, 1H), 7.25 (dd, J = 8.0, 8.0 Hz, 4H), 7.08–7.12 (m, 5H), 7.00–7.04 (m, 3H), 1.84–1.95 (m, 4H), 1.03–1.14 (m, 12H), 0.77 (t, J = 7.1 Hz, 6H), 0.60–0.68 ppm (m, 4H); ^{13}C NMR ($CDCl_3$): δ = 167.2, 157.3, 152.7, 151.8, 148.0, 147.8, 143.2, 140.4, 134.1, 130.4, 129.2, 125.8, 124.2, 123.2, 122.9, 121.8, 120.9, 120.5, 119.7, 118.7, 115.9, 95.8, 55.3, 40.1, 31.5, 29.5, 23.8, 22.5, 14.0 ppm; FAB-MS m/z: 678.3 [M^+]; HRMS: m/z: calcd for $C_{45}H_{46}N_2O_2S$: 678.3280; found: 678.3283 [M^+]; elemental analysis calcd (%) for $C_{45}H_{46}N_2O_2S$: C 79.61, H 6.83, N 4.13; found: C 79.75, H 7.15, N 4.05.

Assembly and characterization of DSSCs: The TiO_2 electrode with a 0.25 cm^2 geometric area was immersed in an acetonitrile/*tert*-butanol mixture (1:1) containing bis(tetrabutyl-ammonium)-*cis*-di(thiocyanato)-*N*,*N*′-bis(4-carboxylato-4′-carboxylic acid-2,2′-bipyridine)ruthenium(II) (3×10^{-4} M, N719, Solaronix S.A., Switzerland) or in a THF solution containing organic sensitizers (3×10^{-4} M) for at least 12 h. A platinized FTO was used as a counter electrode and was controlled to give an active area of 0.36 cm^2 by adhered polyester tape with a thickness of 60 μm. After rinsing with CH_3CN or THF, the photoanode was placed on top of the counter electrode and they were tightly clipped together to form a cell. Electrolyte was then injected into the space and the cell was sealed with Torr Seal cement (Varian, MA, USA). The electrolyte was composed of lithium iodide (LiI, 0.5 M), iodine (I_2, 0.05 M), and 4-*tert*-butylpyridine (TBP, 0.5 M) dissolved in acetonitrile. A 0.6×0.6 cm^2 cardboard mask was clipped onto the device to constrain the illumination area. The photoelectrochemical characterizations on the solar cells were carried out by using a modified light source, a 300 W Xe lamp (Oriel 6258) equipped with a water-based IR filter, and AM 1.5 filter (Oriel 81088). Photocurrent-voltage characteristics of the DSSCs were recorded with a potentiostat/galvanostat (CHI650B, CH Instruments, USA) at a light intensity of 100 mW cm^{-2} measured by a thermopile probe (Oriel 71964). The light intensity was further calibrated by an Oriel reference solar cell (Oriel 91150) and adjusted to be 1.0 sun. The monochromatic quantum efficiency was recorded through a monochromator (Oriel 74100) at short circuit condition. The intensity of each wavelength was in the range of 1 to 3 mW cm^{-2}.

The photovoltage transients of assembled devices were recorded with a digital oscilloscope (LeCroy, WaveSurfer 24Xs). Pulsed laser excitation was applied by a Q-switched Nd:YAG laser (Continuum, model Minilite II) with a 1 Hz repetition rate at 532 nm and a 5 ns pulse width at half height. The beam size was slightly larger than 0.5×0.5 cm^2 to cover the area of the device with an incident energy of 1 mJ cm^{-2}. The recombination lifetime of photoinjected electrons with oxidized dyes was measured by transient photovoltages at open circuit in the presence of $LiClO_4$ or LiI electrolyte (0.5 M). The average electron lifetime can be estimated approximately by fitting a decay of the open circuit voltage transient with $\exp(-t/\tau_R)$, in which t is time and τ_R is an average time constant before recombination.

Computational methodology: Geometrical optimization of the molecules at the density functional level was carried out with Q-Chem[30] software by using the B3LYP exchange-correlation functional and the 6-31G* basis set. The gas-phase time-dependent DFT (TD-DFT) calculations at the same level were performed on the basis of the geometry in the ground state. TD-DFT calculations were previously employed to characterize excited states with charge-transfer character.[31] In some cases, underestimation of the excitation energies was observed.[31,32] Therefore, in the present work, we characterize the electronic configuration and avoid drawing conclusions from the excitation energy.

Acknowledgements

We thank the National Science Council and Academia Sinica for financial support.

[1] a) C. J. Brabec, N. S. Sariciftci, J. C. Hummelen, *Adv. Funct. Mater.* **2001**, *11*, 15–26; b) B. Maennig, J. Drechsel, D. Gebeyehu, P. Simon, F. Kozlowski, A. Werner, F. Li, S. Grundmann, S. Sonntag, M. Koch, K. Leo, M. Pfeiffer, H. Hoppe, D. Meissner, N. S. Sariciftci, I. Riedel, V. Dyakonov, J. Parisi, *Appl. Phys. A* **2004**, *79*, 1–14; c) C. J. Brabec, *Sol. Energy Mater. Sol. Cells* **2004**, *83*, 273–292; d) H. Hoppe, N. S. Sariciftci, *J. Mater. Res.* **2004**, *19*, 1924–1945.

[2] a) A. Hagfeldt, M. Grätzel, *Acc. Chem. Res.* **2000**, *33*, 269–277; b) M. Grätzel, *J. Photochem. Photobiol. C* **2003**, *4*, 145–153; c) M. Grätzel, *Inorg. Chem.* **2005**, *44*, 6841–6851; d) N. Robertson, *Angew. Chem.* **2006**, *118*, 2398–2405; *Angew. Chem. Int. Ed.* **2006**, *45*, 2338–2345.

[3] a) W. Ma, C. Yang, X. Gong, K. Lee, A. J. Heeger, *Adv. Funct. Mater.* **2005**, *15*, 1617–1622; b) J. Hou, H.-Y. Chen, S. Zhang, G. Li, Y. Yang, *J. Am. Chem. Soc.* **2008**, *130*, 16144–16145.

[4] a) M. K. Nazeeruddin, A. Kay, I. Rodicio, R. Humphry-Baker, E. Mueller, P. Liska, N. Vlachopoulos, M. Grätzel, *J. Am. Chem. Soc.* **1993**, *115*, 6382–6390; b) M. Grätzel, *J. Photochem. Photobiol. A* **2004**, *164*, 3–14; c) M. K. Nazeeruddin, F. DeAngelis, S. Fantacci, A. Selloni, G. Viscardi, P. Liska, S. Ito, B. Takeru, M. Grätzel, *J. Am. Chem. Soc.* **2005**, *127*, 16835–16847; d) Y. Chiba, A. Islam, Y. Watanabe, R. Komiya, N. Koide, L. Han, *Jpn. J. Appl. Phys. Part 2* **2006**, *45*, L638–L640; e) F. Gao, Y. Wang, J. Zhang, D. Shi, M. Wang, R. Humphrey-Baker, P. Wang, S. M. Zakeeruddin, M. Grätzel, *Chem. Commun.* **2008**, 2635–2637.

[5] B. O'Reagen, M. Grätzel, *Nature* **1991**, *353*, 737–740.

[6] M. K. Nazeeruddin, P. Péchy, T. Renouard, S. M. Zakeeruddin, R. Humphrey-Baker, P. Comte, P. Liska, L. Cevey, E. Costa, V. Shklover, L. Spiccia, G. B. Deacon, C. A. Bignozzi, M. Grätzel, *J. Am. Chem. Soc.* **2001**, *123*, 1613–1624.

[7] a) P. Wang, S. M. Zakeeruddin, J. E. Moser, R. Humphry-Baker, P. Comte, V. Aranyos, A. Hagfeldt, M. K. Nazeeruddin, M. Grätzel, *Adv. Mater.* **2004**, *16*, 1806–1811; b) M. K. Nazeeruddin, T. Bessho, Le Cevey, S. Ito, C. Klein, F. De Angelis, S. Fantacci, P. Comte, P. Liska, H. Imai, M. Grätzel, *J. Photochem. Photobiol. A* **2007**, *185*, 331–337; c) F. Gao, Y. Wang, J. Zhang, D. Shi, M. Wang, R. Humphrey-Baker, P. Wang, S. M. Zakeeruddin, M. Grätzel, *Chem. Commun.* **2008**, 2635–2637; d) T. Bessho, E. Yoneda, J.-H. Yum, M. Guglielmi, I. Tavernmelli, H. Imai, U. Rothlisberger, M. K. Nazeeruddin, M. Grätzel, *J. Am. Chem. Soc.* **2009**, *131*, 5930–5934; e) J.-H. Yum, I. Jung, C. Baik, J. Ko, M. K. Nazeeruddin, M. Grätzel, *Energy Environ. Sci.* **2009**, *2*, 100–102; f) Y. Cao, Y. Bai, Q. Yu, Y. Cheng, S. Liu, D. Shi, F. Gao, P. Wang, *J. Phys. Chem. C* **2009**, *113*, 6290–6297; g) B.-S. Chen, K. Chen, Y.-H. Hong, W.-H. Liu, T.-H. Li, C.-H. Lai, P.-T. Chou, Y. Chi, G.-H. Lee, *Chem. Commun.* **2009**, 5844–5846.

[8] Y. Tachibana, S. A. Haque, I. P. Mercer, J. R. Durant, D. R. Klug, *J. Phys. Chem. B* **2000**, *104*, 1198–1205.

[9] A. Mishra, M. K. R. Fischer, P. Bäuerle, *Angew. Chem.* **2009**, *121*, 2510–2536; *Angew. Chem. Int. Ed.* **2009**, *48*, 2474–2499.

[10] G. Zhang, H. Bala, Y. Cheng, D. Shi, X. Lv, Q. Yu, P. Wang, *Chem. Commun.* **2009**, 2198–2200.

[11] a) K. Hara, K. Sayama, Y. Ohga, A. Shinpo, S. Suga, H. Arakawa, *Chem. Commun.* **2001**, 569–570; b) K. Hara, M. Kurashige, Y. Danoh, C. Kasada, A. Shinpo, S. Suga, K. Sayama, H. Arakawa, *New J. Chem.* **2003**, *27*, 783–785.

[12] a) T. Horiuchi, H. Miura, S. Uchida, *Chem. Commun.* **2003**, 3036–3037; b) T. Horiuchi, H. Miura, S. Uchida, *J. Photochem. Photobiol. A* **2004**, *164*, 29–32; c) T. Horiuchi, H. Miura, K. Sumioka, S. Uchida, *J. Am. Chem. Soc.* **2004**, *126*, 12218–12219; d) S. Ito, S. M. Zakeeruddin, R. Humphry-Baker, P. Liska, R. Charvet, P. Comte, M. K. Nazeeruddin, P. Péchy, M. Takata, H. Miura, S. Uchida, M. Grätzel, *Adv. Mater.* **2006**, *18*, 1202–1205.

[13] A. Ehret, L. Stuhl, M. T. Spitler, *J. Phys. Chem. B* **2001**, *105*, 9960–9965.

[14] a) Z.-S. Wang, F.-Y. Li, C.-H. Huang, *Chem. Commun.* **2000**, 2063–2064; b) Q.-H. Yao, F.-S. Meng, F.-Y. Li, H. Tian, C.-H. Huang, *J. Mater. Chem.* **2003**, *13*, 1048–1053.

[15] a) A. C. Khazraji, S. Hotchandani, S. Das, P. V. Kamat, *J. Phys. Chem. B* **1997**, *101*, 4693–4700; b) K. Sayama, K. Hara, N. Mori, M. Satsuki, S. Suga, S. Tsukagoshi, Y. Abe, H. Sughara, H. Arakawa, *Chem. Commun.* **2000**, 1173–1174; c) K. Sayama, S. Tsukagoshi, T. Mori, K. Hara, Y. Ohga, A. Shinpou, Y. Abe, S. Suga, H. Arakawa, *Sol. Energy Mater. Sol. Cells* **2003**, *80*, 47–71.

[16] a) S. Ferrere, A. Zaban, B. A. Gregg, *J. Phys. Chem. B* **1997**, *101*, 4490–4493; b) S. Ferrere, B. A. Gregg, *New J. Chem.* **2002**, *26*, 1155–1160.

[17] a) M. Velusamy, K. R. J. Thomas, J. T. Lin, Y.-C. Hsu, K.-C. Ho, *Org. Lett.* **2005**, *7*, 1899–1902; b) K. R. J. Thomas, J. T. Lin, Y.-C. Hsu, K.-C. Ho, *Chem. Commun.* **2005**, 4098–4100; c) D. P. Hagberg, T. Edvinsson, T. Marinado, G. Boschloo, A. Hagfeldt, L. Sun, *Chem. Commun.* **2006**, 2245–2247; d) S.-L. Li, K.-J. Jiang, K.-F. Shao, L.-M. Yang, *Chem. Commun.* **2006**, 2792–2794; e) N. Koumura, Z.-S. Wang, S. Mori, M. Miyashita, E. Suzuki, K. Hara, *J. Am. Chem. Soc.* **2006**, *128*, 14256–14257; f) S. Kim, J. K. Lee, S. O. Kang, J. Ko, J.-H. Yum, S. Fantacci, F. De Angelis, D. Di Censo, M. K. Nazeeruddin, M. Grätzel, *J. Am. Chem. Soc.* **2006**, *128*, 16701–16707; g) K. R. J. Thomas, Y.-C. Hsu, J. T. Lin, K.-M. Lee, K.-C. Ho, C.-H. Lai, Y.-M. Cheng, P.-T. Chou, *Chem. Mater.* **2008**, *20*, 1830–1840.

[18] a) M. Liang, W. Wu, F. Cai, P. Chen, B. Peng, J. Chen, Z. Li, *J. Phys. Chem. C* **2007**, *111*, 4465–4472; b) H. Choi, J. K. Lee, K. Song, S. O. Kang, J. Ko, *Tetrahedron* **2007**, *63*, 3115–3121; c) I. Jung, J. K. Lee, K. H. Song, K. Song, S. O. Kang, J. Ko, *J. Org. Chem.* **2007**, *72*, 3652–3658; d) S.-T. Huang, Y.-C. Hsu, Y.-S. Yen, H.-H. Chou, J. T. Lin, C.-W. Chang, C.-P. Hsu, C. Tsai, D.-J. Yin, *J. Phys. Chem. C* **2008**, *112*, 19739–19747; e) Z. Ning, H. Tian, *Chem. Commun.* **2009**, 5483–5495; f) Z. Ning, Q. Zhang, H. Pei, J. Luan, C. Lu, Y. Cui, H. Tian, *J. Phys. Chem. C* **2009**, *113*, 10307–10313.

[19] a) Y.-K. Wang, C.-F. Shu, E. M. Breitung, R. J. McMahon, *J. Mater. Chem.* **1999**, *9*, 1449–1452; b) P. R. Varanasi, A. K.-Y. Jen, J. Chandrasekhar, I. N. N. Namboothiri, A. Rathna, *J. Am. Chem. Soc.* **1996**, *118*, 12443–12448.

[20] K. R. J. Thomas, M. Velusamy, J. T. Lin, C.-H. Chuen, Y.-T. Tao, *Chem. Mater.* **2005**, *17*, 1860–1866.

[21] K. Hara, T. Sato, R. Katoh, A. Furube, Y. Ohga, A. Shinpo, S. Suga, K. Sayama, H. Sugihara, H. Arakawa, *J. Phys. Chem. B* **2003**, *107*, 597–606.

[22] A. Hagfeldt, M. Grätzel, *Chem. Rev.* **1995**, *95*, 49–68.

[23] A. Baheti, P. Tyagi, K. R. J. Thomas, Y.-C. Hsu, J. T. Lin, *J. Phys. Chem. C* **2009**, *113*, 8541–8547.

[24] Y. J. Chang, T. J. Chow, *Tetrahedron* **2009**, *65*, 4726–4734.

[25] a) D. P. Hagberg, T. Marinado, K. M. Karlsson, K. Nonomura, P. Qin, G. Boschloo, T. Brinck, A. Hagfeldt, L. Sun, *J. Org. Chem.* **2007**, *72*, 9550–9556; b) W.-H. Liu, I.-C. Wu, C.-H. Lai, C.-H. Lai, P.-T. Chou. Y.-T. Li, C.-L. Chen, Y.-Y. Hsu, Y. Chi, *Chem. Commun.* **2009**, 5152–5154.

[26] a) L. Schmidt-Mende, M. Grätzel, *Thin Solid Films* **2006**, *500*, 296–301; b) H. J. Snaith, A. J. Moule, C. Klein, K. Meerholz, R. H. Friend, M. Grätzel, *Nano Lett.* **2007**, *7*, 3372–3376; c) H. J. Snaith, C. S. Karthikeyan, A. Petrozza, J. Teuscher, J. E. Moser, Md. K. Nazeeruddin, M. Thelakkat, M. Grätzel, *J. Phys. Chem. C* **2008**, *112*, 7562–7566.

[27] a) J.-J. Cid, J.-H. Yum, S.-R. Jang, Md. K. Nazeeruddin, E. Martínez-Ferrero, E. Palomares, J. Ko, M. Grätzel, T. Torres, *Angew. Chem.* **2007**, *119*, 8510–8514; *Angew. Chem. Int. Ed.* **2007**, *46*, 8358–8362; b) H. Choi, S. Kim, S. O. Kang, J. Ko, M.-S. Kang, J. N. Clifford, A. Forneli, E. Palomares, Md. K. Nazeeruddin, M. Grätzel, *Angew. Chem.* **2008**, *120*, 8383–8387; *Angew. Chem. Int. Ed.* **2008**, *47*, 8259–8263.

[28] a) H. Ishii, K. Sugiyama, E. Ito, K. Seki, *Adv. Mater.* **1999**, *11*, 605–625; b) S. Braun, W. R. Salaneck, M. Fahlman, *Adv. Mater.* **2009**, *21*, 1450–1472.

[29] S. Rühle, M. Greenshtein, S.-G. Chen, A. Merson, H. Pizem, C. S. Sukenik, D. Cahen, A. Zaban, *J. Phys. Chem. B* **2005**, *109*, 18907–18913.

[30] a) N. Hirata, J.-J. Lagref, E. J. Palomares, J. R. Durrant, M. K. Nazeeruddin, M. Grätzel, D. Di Censo, *Chem. Eur. J.* **2004**, *10*, 595–602; b) J. R. Durrant, S. A. Haque, E. Palomares, *Chem. Commun.* **2006**, 3279–3289; c) Y. Shao, L. F. Molnar, Y. Jung, J. Kussmann, C. Ochsenfeld, S. T. Brown, A. T. B. Gilbert, L. V. Slipchenko, S. V. Levchenko, D. P. O'Neill, R. A. Jr DiStasio, R. C. Lochan, T. Wang, G. J. O. Beran, N. A. Besley, J. M. Herbert, C. Y. Lin, T. V. Voorhis, S. H. Chien, A. Sodt, R. P. Steele, V. A. Rassolov, P. E. Maslen, P. P. Korambath, R. D. Adamson, B. Austin, J. Baker, E. F. C. Byrd, H. Dachsel, R. J. Doerksen, A. Dreuw, B. D. Dunietz, A. D. Dutoi, T. R. Furlani, S. R. Gwaltney, A. Heyden, S. Hirata, C.-P. Hsu, G. Kedziora, R. Z. Khalliulin, P. Klunzinger, A. M. Lee, M. S. Lee, W. Z. Liang, I. Lotan, N. Nair, B. Peters, E. I. Proynov, P. A. Pieniazek, Y. M. Rhee, J. Ritchie, E. Rosta, C. D. Sherrill, A. C. Simmonett, J. E. Subotnik, H. L. III Woodcock, W. Zhang, A. T. Bell, A. K. Chakraborty, *Phys. Chem. Chem. Phys.* **2006**, *8*, 3172–3191.

[31] a) H. M. Vaswani, C.-P. Hsu, M. Head-Gordon, G. R. Fleming, *J. Phys. Chem. B* **2003**, *107*, 7940–7946; b) Y. Kurashige, T. Nakajima, S. Kurashige, K. Hirao, Y. Nishikitani, *J. Phys. Chem. A* **2007**, *111*, 5544–5548.

[32] A. Dreuw, M. Head-Gordon, *J. Am. Chem. Soc.* **2004**, *126*, 4007–4016.

Received: November 17, 2009
Published online: January 29, 2010

